


## AUTHOR QUERY FORM

 <b>ELSEVIER</b>	<b>Journal: MSA</b>  <b>Article Number: 28949</b>	<b>Please e-mail or fax your responses and any corrections to:</b>  <b>E-mail: <a href="mailto:corrections.eseo@elsevier.macipd.com">corrections.eseo@elsevier.macipd.com</a></b>  <b>Fax: +44 1392 285878</b>
------------------------------------------------------------------------------------------------------	---------------------------------------------------------	----------------------------------------------------------------------------------------------------------------------------------------------------------------------------------------------------------------------------

Dear Author,

Please check your proof carefully and mark all corrections at the appropriate place in the proof (e.g., by using on-screen annotation in the PDF file) or compile them in a separate list. Note: if you opt to annotate the file with software other than Adobe Reader then please also highlight the appropriate place in the PDF file. To ensure fast publication of your paper please return your corrections within 48 hours.

For correction or revision of any artwork, please consult <http://www.elsevier.com/artworkinstructions>.

Any queries or remarks that have arisen during the processing of your manuscript are listed below and highlighted by flags in the proof. Click on the [Q](#) link to go to the location in the proof.

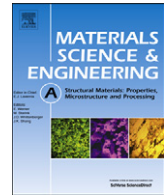
Location in article	Query / Remark: <a href="#">click on the Q link to go</a> Please insert your reply or correction at the corresponding line in the proof
<a href="#">Q1</a>	Please confirm that given names and surnames have been identified correctly and are presented in the desired order.
<a href="#">Q2</a>	Please check the e-mail address of the corresponding author, and correct if necessary.
<a href="#">Q3</a>	Please check the edits made in the legends of Fig. 14, and correct if necessary.

Thank you for your assistance.

Please check this box if you have no corrections to make to the PDF file

Contents lists available at [SciVerse ScienceDirect](http://www.sciencedirect.com)

## Materials Science &amp; Engineering A

journal homepage: [www.elsevier.com/locate/msea](http://www.elsevier.com/locate/msea)

# Influence of rivet to sheet edge distance on fatigue strength of self-piercing riveted aluminium joints

Q1 **Dezhi Li**<sup>a,\*</sup>, **Li Han**<sup>b</sup>, **Martin Thornton**<sup>a</sup>, **Mike Shergold**<sup>b</sup>

<sup>a</sup> Warwick Manufacturing Group, University of Warwick, Coventry CV4 7AL, UK

<sup>b</sup> Jaguar Engineering Centre, Jaguar Land Rover, Coventry CV3 4LF, UK

## ARTICLE INFO

## Article history:

Received 2 May 2012

Received in revised form

24 July 2012

Accepted 30 July 2012

## Keywords:

Self-piercing riveting

Lap shear

Coach peel

Fatigue

## ABSTRACT

Self-piercing riveting (SPR) is one of the main joining methods for lightweight aluminium automotive body structures due to its advantages. In order to further optimise the structure design and reduce the weight but without compromising strength, reduction of redundant materials in the joint flange area can be considered. For this reason, the influence of rivet to sheet edge distance on the fatigue strengths of self-piercing riveted joints was studied. Five edge distances, 5 mm, 6 mm, 8 mm, 11.5 mm and 14.5 mm, were considered. The results showed that the SPR joints studied in this research had high fatigue resistance and all specimens failed in sheet material along joint buttons or next to rivet heads. For lap shear fatigue tests, specimens failed in the bottom sheet at low load amplitudes and in the top sheet at high load amplitudes except for specimens with very short edge distance of 5 and 6 mm; whereas, for coach-peel fatigue tests, all specimens failed in the top sheet. For both lap shear and coach-peel fatigue tests, specimens with an edge distance of 11.5 mm had the best fatigue resistance. It was found that for coach-peel fatigue, length of crack developing path before specimens lost their strengths was the main factor that determined the fatigue life of different specimens; for lap shear fatigue, the level of stress concentration and subsequent crack initiation time was the main factor that determined the fatigue life.

© 2012 Published by Elsevier B.V.

## 1. Introduction

Due to the government legislations on CO<sub>2</sub> emission, aluminium (Al) and high strength steel are increasingly used in automotive body structures to reduce weight for better fuel efficiency and less CO<sub>2</sub> emission. Resistance spot welding is being used as a major joining method for steel body vehicles for many years, but to join Al to Al, resistance spot welding faces some challenges, such as surface sensitivity and short electrode tip life. Resistance spot welding is not suitable for joining Al to steel, since the melting temperatures of Al and steel are not close enough. SPR has been one of the main joining methods for aluminium automotive body structures due to its advantages, such as ability to join similar and dissimilar materials, no pre-drilled holes or alignment required, low energy requirement and high static and fatigue joint strengths [1,2]. Researchers have studied the influence of specimen dimensions on resistance spot welded (RSW) steel joints. Zhou et al. [3] examined lap shear specimens using mild steel specimens with various dimensions and thicknesses. Through experiments and FEA simulation, they suggested that

specimen dimensions not only had a significant effect on the joint strength, but also on joint failure mode. The most influential factor was found to be the specimen width, rather than overlap or length. Similar results were also obtained on RSW high strength steel DP600 by Yang et al. [4] through an experiment study using the same standards as for Zhou et al. However, for SPR, no results on the influence of specimen dimensions have been published. In the previous paper by the authors, the influence of the distance between rivet centre and sheet edge (edge distance) on lap shear and coach-peel static strengths was studied [5], and in the current paper, the influence of edge distance on lap shear and coach-peel fatigue strengths is reported. The results obtained can be used to optimise structure design with respect to flange distance and help to further reduce the vehicle weight.

## 2. Experimental procedure

### 2.1. Materials

The material used in this study is a commercially available 2.0 mm thick AA5754 with a standard pretreatment (PT2) and wax lubricant (AL070). The compositions and mechanical properties of AA5754 are listed in Table 1.

\* Corresponding author. Tel.: +44 2476574614; fax: +44 2476575366.  
E-mail addresses: [dezhilee@hotmail.co.uk](mailto:dezhilee@hotmail.co.uk), [dezhi.li@warwick.ac.uk](mailto:dezhi.li@warwick.ac.uk) (D. Li).

**Table 1**  
Nominal compositions and mechanical properties of AA5754 (balance Al).

Mg	Mn	Cu	Fe	Si	Ti	Cr	Zn	Others
<i>Nominal compositions (balance Al) (wt%)</i>								
2.6–3.6	0–0.5	0–0.1	0–0.4	0–0.4	0–0.15	0–0.3	0–0.2	0–0.15
<i>Mechanical properties</i>								
Hardness (Hv)	UTS (MPa)	0.2% yield strength (MPa)	Elongation (%)					
63.5	241	110	25					

**Table 2**  
Optimum SPR parameters for (2+2)AA5754 stack-up.

Rivet	Length: 6.5 mm; type: countersunk; hardness: ~410 Hv
Die	Cavity diameter: 9 mm; cavity depth: 2 mm; type: flat bottom
Velocity	100 (Henrob unit, determining applied force)

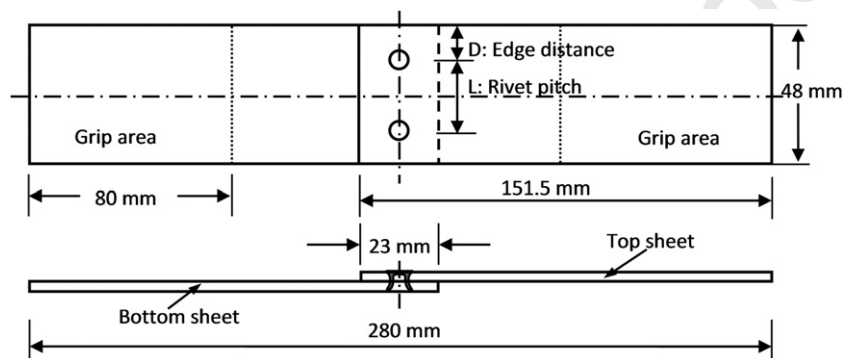


**Fig. 1.** Specimen geometry for lap shear tests.

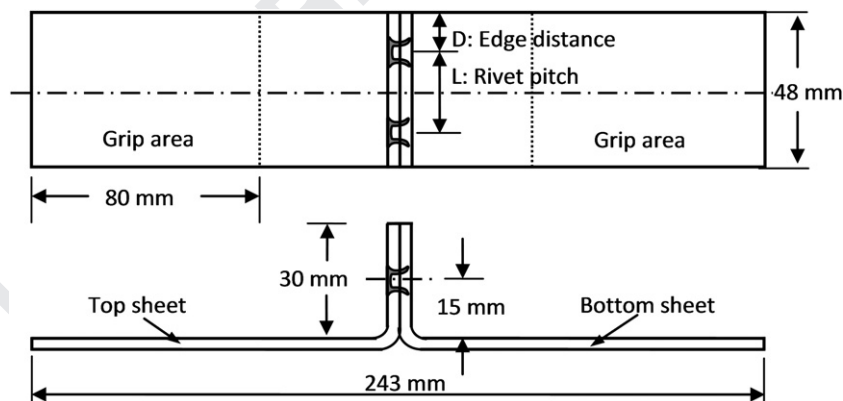


**Fig. 2.** Specimen geometry for coach-peel tests.

## 2.2. Sample preparation

For all stacks, steel rivets with a countersunk head and mechanical zinc/tin surface coating were used. The rivets were supplied by Henrob Ltd., and all samples were produced using a Henrob servo-driven riveting equipment. A rivet/die/velocity combination, as listed in Table 2, was selected to achieve good joint quality.

Specimen geometries and dimensions for lap shear and coach-peel tests are shown in Figs. 1 and 2. During the preparation of specimens, coupons were cut from sheet such that the longitudinal direction of coupons (loading direction during following mechanical tests) coincides with the rolling direction of sheet metal. To study the influence of edge distance on the mechanical strength of SPR joints, specimens with different edge distances, i.e. 5 mm, 6 mm, 8 mm, 11.5 mm and 14.5 mm, as shown in

**Table 3**  
Rivet locations of different edge distance specimens.

Group no.	Rivet pitch $L$ (mm)	Edge distance $D$ (mm)
1	19	14.5
2	25	11.5
3	32	8
4	36	6
5	38	5

Table 3, were studied. To reduce any variations of rivet position, custom designed fixtures were used to set rivets into correct positions. For each specimen, the coupon width was fixed at 48 mm, and two rivets were set with specific edge distance by using the custom fixture.

### 2.3. Mechanical tests and joint quality analysis

Custom designed lightweight aluminium grips were used for fatigue tests to reduce inertia and increase fatigue machine's response speed. These grips were specially designed for lap shear fatigue tests so that the gripping surfaces of the two fixed jaws from the upper and lower grips (in opposite sides) were aligned along the joint interface, with no spacers needed. When the two fixed jaws were turned to the same side, in combination with internal spacers, the same grips can also be used for coach-peel fatigue tests. Load-controlled fatigue tests were performed on a close-loop servo hydraulic testing machine using a sinusoidal waveform and in tension-tension mode. The ratio of the minimum load and the maximum load or  $R$  ratio was 0.1 and the test frequency was 15 Hz in all the tests. Three or four load levels, with different values of maximum load or load amplitude (half of the difference between maximum load and minimum load) were used in the tests. The maximum loads for fatigue were determined according to the maximum loads obtained through static tests. For lap shear, the values of the maximum loads used were about 30–80% of the maximum loads obtained from static tests. As the maximum loads that could be sustained in coach-peel fatigue were much lower than those in static tests, 20–50% of the maximum loads obtained from static tests were used. The failure criterion for fatigue was fracture of the specimens. Some specimens were terminated in the middle of fatigue at different stages and cross-sectioned for crack initiation and growth study.

Joint quality of specimens (not fatigue tested) with each edge distance was inspected through cross-sections. A special fixture was used to ensure that all joints were vertically cross-sectioned through the centre of the rivets in transverse direction. Following sectioning, the joint features were measured and analysed with respect to rivet head height, interlock and remaining bottom material thickness using a 4i image analysis software, a dedicated image capture, archive, analysis and data basing package supplied by Aquinto. Some of the fracture interfaces were analysed through a Zeiss Sigma SEM.

## 3. Results

### 3.1. Influence of edge distance on joint quality

Fig. 3 shows the cross-sections of SPR joints (not fatigue tested) with different edge distances. The symmetrical nature of

the specimens means it is only necessary to show one rivet section. For each case one rivet joint from the same side is shown. Measurements made from the cross sections show that the joint qualities, in terms of rivet head height, interlock and minimum remaining bottom material thickness, were similar. However, it was observed that the behaviour of specimen edge, during the rivet setting process, was affected by the edge distance. Depending upon edge distance, the extent that the bottom sheet was drawn into the die cavity varied; when the edge distance was not less than 8.0 mm, no obvious bottom sheet contraction was observed, as shown in Fig. 3a–c; further reduction in the edge distance caused the bottom sheet to be drawn towards the die, which was evident by the step generated between the top and bottom sheets.

During the SPR process, a small circular area of each sheet is held between a blank holder and a die forming a constrained area. Depending on the die profile (diameter, depth and pip shape and height), these constrained areas are deformed by rivet piercing and flaring into the die cavity to form mechanical interlocks with certain integrity. The Henrob riveting gun used for this study has a blank holder and a die with 18 mm outer diameters (effective holding diameter is about 16 mm, if the radius of outer edge is considered), which means that sufficient minimum edge distance is around 8.0 mm. For edge distances greater than 8.0 mm, both sheets can be clamped efficiently and therefore are constrained from being drawn into the die cavity leading to no obvious edge contraction. However, when the edge distance is reduced, the efficiency to grip the sheets between the blank holder and die is reduced leading to easier movement of material; and the available material that can be deformed into the die cavity is also limited. Therefore, small edge distances lead to greater contraction of the edge materials, as indicated in Fig. 3d and e. For any SPR joints, the bottom sheet is always deformed more than the top sheet, as it is drawn into the die profile during rivet flaring; whilst the top sheet is pierced through by the rivet.

### 3.2. Influence of edge distance on fatigue strength

Fig. 4 shows the lap shear fatigue  $S-N$  curves for specimens with different edge distances. It can be seen that with the increase of edge distance up to 11.5 mm the fatigue life of specimens was increasing. Around the edge distance of 11.5 mm, the fatigue life of specimens reached maximum value and when edge distance

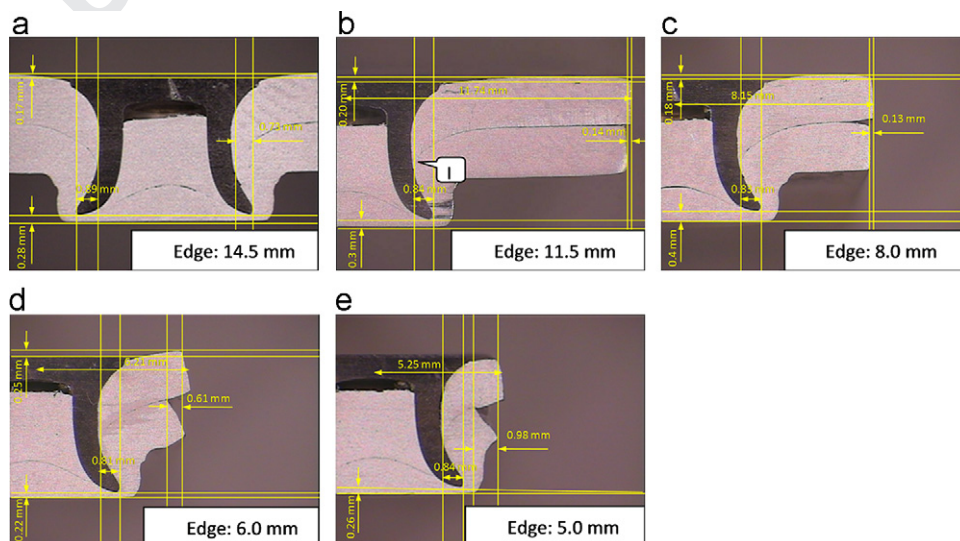


Fig. 3. Cross-sections of SPR joints along rivet centre and transverse direction with different edge distances.

increased further to 14.5 mm, the fatigue life of specimens began to drop slightly. Fig. 4 also shows that there are two large differences as to fatigue life between 5 mm and 6 mm edge distances and 6 mm and 8 mm edge distances. It can also be seen that the slope of the fitted line for 6 mm edge distance specimen is different from the others. The results show that when the edge distance changed from 5 mm to 6 mm, the fatigue life of specimens in high load amplitude or low cycle end increased much more than that in low load amplitude or high cycle end and that, when the edge distance changed from 6 mm to 8 mm the fatigue life of specimens in low load amplitude end increased much more than that in high load amplitude end. For other edge distance differences, the influence of edge distance on high and low cycle ends was similar.

Lap shear fatigue life data showed that the fatigue life of specimens with edge distance of 11.5 mm was 5–8 times of that of specimens with edge distance of 5 mm and 1.4–1.7 times of that of specimens with edge distance of 8 mm, at different load amplitudes.

Fig. 5 shows the coach-peel fatigue  $S-N$  curves for specimens with different edge distances. It can be seen that the fatigue life of specimens with edge distances of 5 mm and 6 mm was almost identical, but when edge distance increased from 6 mm to 8 mm and 11.5 mm, the fatigue life of specimens had an obvious increase. Around the edge distance of 11.5 mm, the fatigue life of specimens reached maximum value and when edge distance increased further to 14.5 mm, the fatigue life of specimens began to drop slightly. Fig. 5 also shows that the slopes of the fitted line

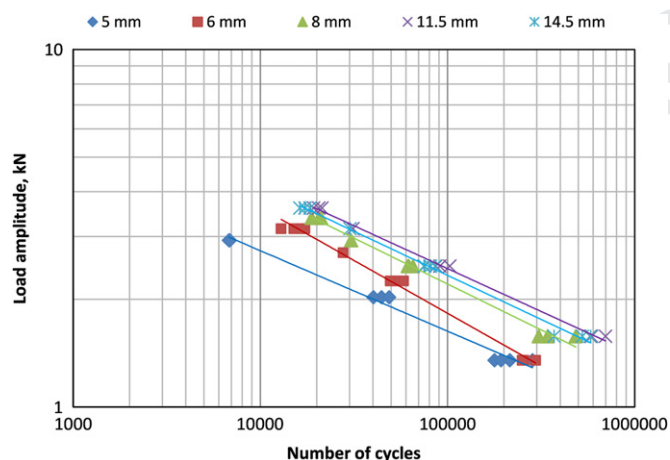


Fig. 4. Lap shear fatigue  $S-N$  curves for specimens with different edge distances.

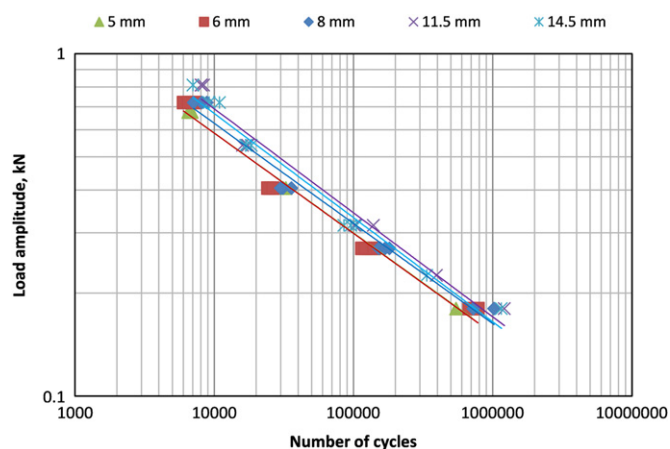


Fig. 5. Coach-peel fatigue  $S-N$  curves for specimens with different edge distances.

are similar, which means that the influence of specimen edge distance on the fatigue life in high cycle and low cycle ends were of the same manner.

Coach-peel fatigue life data showed that the fatigue life of specimens with edge distance of 11.5 mm was around 1.6 times that of specimens with edge distance of 5 mm and around 1.4 times of specimens with edge distance 8 mm at different load amplitudes. Compared with the influence of edge distance on the lap shear fatigue life, it can be seen that the influence of edge distance on coach-peel fatigue life was more benign.

Based on the lap shear and coach-peel fatigue results, it can be seen that to achieve an acceptable lap shear and coach-peel fatigue performance the minimum edge distance needs to be not less than 8 mm.

## 4. Discussion

### 4.1. Failure modes

For the stack and joints studied in this paper, during static tests, specimens failed by rivets being pulled out from either bottom or top sheet or simultaneously from both sheets [5]; however, during fatigue tests, because the maximum loads applied were not enough to pull rivets out, and the substrates (top and bottom sheet materials) were continuously subjected to cyclic bending, all specimens failed in substrate sheet materials.

Table 4 shows the failure modes of specimens with different edge distances and at different load amplitudes. For specimens with edge distance of 5 mm, all specimens tested failed in the bottom sheet along joint buttons. For specimens with edge distance of 6 mm, the specimen tested at the low load amplitude failed in the bottom sheet along joint buttons, but with the increase of load amplitudes, specimens started to fail partially in bottom and top sheets with the main failure locations transferring from bottom sheet to top sheet. Specimens with edge distances of 8–14.5 mm, tested at the low load amplitude, failed in the bottom sheet along joint buttons; whilst those tested at higher load amplitudes failed in the top sheet next to the rivet heads.

Table 4

Failure modes of specimens with different edge distances and at different load amplitudes.

Edge distance (mm)	Maximum load/load amplitude (kN)	Failure modes
5	3/1.35	Bottom sheet along joint buttons
	4.5/2.025	Bottom sheet along joint buttons
	6.5/2.925	Bottom sheet along joint buttons
6	3/1.35	Bottom sheet along joint buttons
	5/2.25	Bottom sheet along joint buttons and top sheet next to rivet heads (more failure from bottom sheet)
	7/3.15	Bottom sheet along joint buttons and top sheet next to rivet heads (more failure from top sheet)
8	3.5/1.575	Bottom sheet along joint buttons
	5.5/2.475	Top sheet next to rivet heads
	7.5/3.375	Top sheet next to rivet heads
11.5	3.5/1.575	Bottom sheet along joint buttons
	5.5/2.475	Top sheet next to rivet heads
	8/3.6	Top sheet next to rivet heads
14.5	3.5/1.575	Bottom sheet along joint buttons
	5.5/2.475	Top sheet next to rivet heads
	8/3.6	Top sheet next to rivet heads

Fig. 6 shows the lap shear fatigue fracture interfaces of specimens with different edge distances tested at low load amplitudes. It can be seen that all specimens failed in the bottom sheet along the joint buttons. For specimens with edge distance from 5 mm to 8 mm, because the final connection areas before failure were located at the centre of bottom sheets, the free end of the bottom sheet was deformed into a concave shape. However, for specimens with edge distance of 11.5 mm, because the specimens almost simultaneously failed at centre and edges of bottom sheets, the free end of the bottom sheet was still flat. Consequently, for specimens with edge distance of 14.5 mm, because the final connection areas before failure were at the two edge areas, the free end of the bottom sheet was deformed into a convex shape.

Fig. 7 shows the lap shear fatigue fracture interfaces of specimens with different edge distances tested at higher load amplitudes. It can be seen that specimens with edge distance from 8 mm to 14.5 mm failed in the top sheet next to rivet heads. For the same reason as for low load amplitudes, the free ends of the top sheet were deformed into a concave, flat and convex shape for specimens with edge distances of 8 mm, 11.5 mm and 14.5 mm, respectively.

For specimens with edge distance of 5 mm, the areas between joint buttons and sheet edges in the bottom sheet were so weak that all specimens failed in bottom sheet, across joint buttons, even in high load amplitudes. This occurs because of the

contraction of the bottom sheets during the SPR process as shown in Fig. 3. For specimens with edge distance of 6 mm, at higher load amplitudes, all specimens failed in both top sheet next to rivet heads and bottom sheet across joint buttons, as shown in Fig. 8. From Table 3, it can be seen that with the increase of load amplitudes, a greater portion of failure would occur in the top sheet next to rivet heads.

When a specimen is under lap shear tests, it will be subjected to tension and secondary bending [6,7]. There will be a larger deformation and higher bending amplitude for higher applied loads. Unlike static tests, in which rivets were pulled out either from a top or a bottom sheet or simultaneously from both top and bottom sheet for the stack and joints studied, in a fatigue test, specimens always failed from top and/or bottom sheet, and cyclic secondary bending was the main reason for the failure. During the SPR joining process, the deformation of the bottom sheet was much larger than that of the top sheet, because the top sheet was just punched a hole but the bottom sheet was stretched into the die cavity. As a result, the residual stress/strain in the bottom sheet around a joint button was much higher than that of the material in the top sheet around the punched hole. It is believed that this large residual strain reduced the fatigue life of the bottom sheet material around a joint button at low applied load amplitudes and the combination of secondary bending and local residual strain caused the failure along joint button. The influence of deformation during the joining process on fatigue life is similar

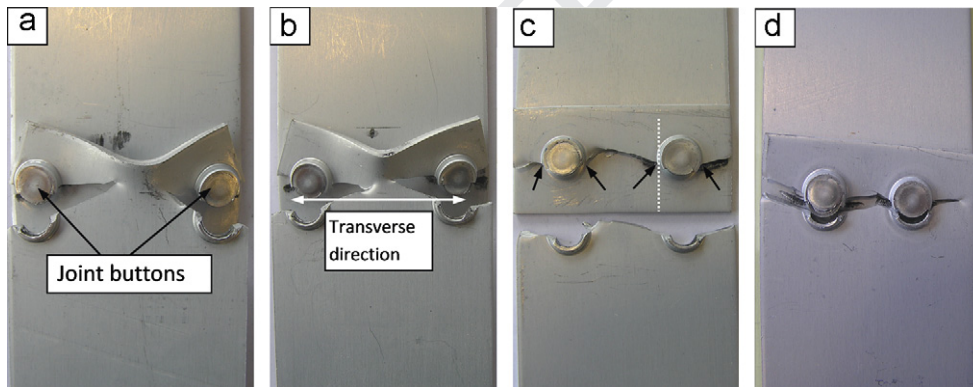


Fig. 6. Lap shear fatigue fracture interfaces of specimens tested at low load amplitudes, 1.35 kN or 1.575 kN, for specimen with different edge distances: (a) 6 mm, (b) 8 mm, (c) 11.5 mm and (d) 14.5 mm.

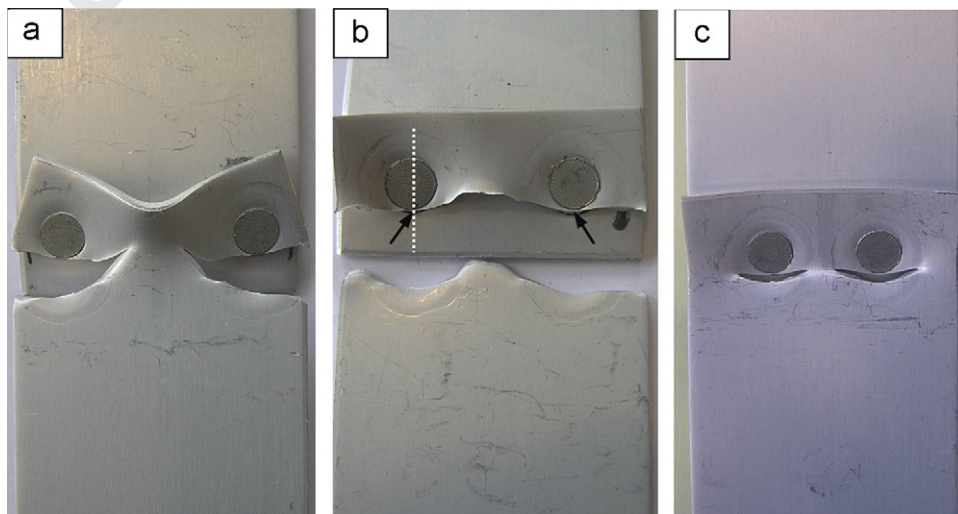


Fig. 7. Lap shear fatigue fracture interfaces of specimens tested at higher load amplitudes, 2.025–3.6 kN, for specimen with different edge distances: (a) 8 mm, (b) 11.5 mm and (c) 14.5 mm.

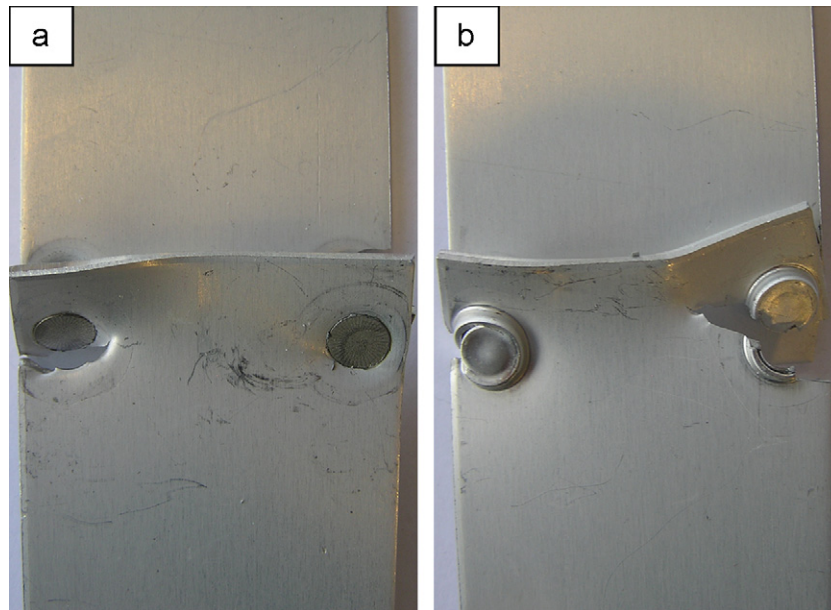


Fig. 8. Lap shear fatigue fracture interfaces for specimen with 6 mm edge distance at load amplitude not less than 2.25 kN: (a) top view, and (b) bottom view.

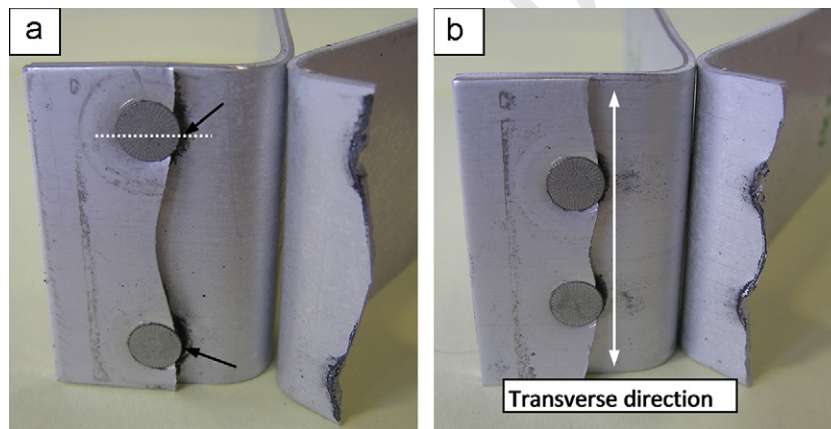


Fig. 9. Coach-peel fatigue fracture interfaces for specimens with different edge distances: (a) 8 mm and (b) 14.5 mm.

with that of prestain and this influence is consistent with the result from Kalluri et al. [8]. In their study, they found that prestain could significantly reduce the fatigue of Inconel 718 in the low stress/high cycle range. At high applied load amplitudes, the influence of prestain on fatigue life is believed not significant. Due to the pivot function of the outer edge of rivet head during higher amplitude secondary bending, a large stress was concentrated at the bottom surface of top sheet roughly underneath the outer ring of rivet head, and as a result, all joints with edge distance larger than 8 mm failed in the top sheet next to rivet head. Research from Chen et al. [9] and Han et al. [10] showed that the fretting at sheet interface of SPR joints caused fretting damage, stress concentration and subsequent fatigue cracks. In this study, although the stress concentration caused by secondary bending with the outer edge of rivet head as the pivot was the main reason for fatigue failure at high applied load amplitudes, it was possible that the fretting at the joint interface facilitated and accelerated the crack initiation and development. The different stress concentration levels and locations, at higher and lower amplitudes fatigue, may be another reason that caused the different failures observed. When specimens were tested at high applied load amplitudes, all specimens with edge distance of 5 mm failed in the bottom sheet along joint buttons and all

specimens with edge distance of 6 mm failed partially in the bottom sheet along joint buttons and partially in the top sheet next to rivet heads. This is believed to be caused by the very narrow and weak areas between the rivet and sheet edges. When edge distances were small, such as 5 mm and 6 mm, because the joint buttons had a diameter of 9 mm, the edges of joint buttons were very close (about 0.5 and 1.5 mm, respectively) to edges of sheet material, leaving the areas between the bottom sheet edges and rivets very weak. For specimens with edge distance of 5 mm, the areas between rivets and bottom sheet edges were weaker than those between rivets and top sheet edges, and for specimens with edge distance of 6 mm, the strength of these two locations were similar.

Fig. 9 shows the typical coach-peel fatigue fracture interfaces for specimens with different edge distances. For coach-peel fatigue tests, the failure modes were the same for all specimens with failure in the top sheets, over the complete range of load amplitudes.

Cyclic bending was the main reason for the fatigue failure of coach-peel specimens. Because of the geometry and the loading direction, during a fatigue test, the bending amplitude was much larger than the maximum bending amplitude in a lap shear fatigue test even with low applied load amplitude. It is believed





amplitude, which failed in the top sheet next to rivet heads. Fig. 12a shows the microstructure of the crack initiation areas. The intergranular fracture interface indicated that cracks initiated along grain boundaries. From Fig. 12a, one can also see that the intergranular fracture distance was small, about 40–60  $\mu\text{m}$  along the sheet thickness direction, and after crack initiation, the crack development along the sheet thickness direction changed to transgranular fracture. For the transverse direction (sheet width direction), the intergranular fracture distance was larger, about 2 mm, before changing to transgranular fracture. This difference in thickness and width directions might be caused by multicrack initiation points and uneven stress distribution along these two directions. Fig. 12b and c shows the microfracture interfaces during the stage II crack growth process, at the locations marked in Fig. 11: areas B and C, respectively. It can be seen that the interface failed by transgranular fracture and in the later stage of crack growth the fatigue striation marks became more obvious and the distance between the two adjacent marks became larger because the crack growth rate was increasing with the crack development. Fig. 12d presents the fracture interface due to final fracture after the local stress exceeded the fracture strength of the remaining structure, from which a ductile fracture interface with lots of dimples can be seen.

As mentioned above, when specimens were fatigue tested with low load amplitude, they failed in the bottom sheets along joint buttons. The microstructure of the fracture interfaces was similar to those shown in Fig. 12. During these fatigue tests, cracks initiated at the intersections of the secondary bending line and the partially pierced holes of the bottom sheet, as marked in Fig. 9b by arrows. Then cracks would grow from transverse directions: along the thinnest areas of joint buttons (ring shape due to the penetration of rivet skirts) on one side and along the bulk sheet to the edges or centre on the other side. Cracks also grew along the sheet thickness direction. Finally, when the remaining structure could no longer sustain the load applied, sudden fracture occurred. For a different joint geometry, for

example, a joint with very thin remaining bottom material, the cracking along the thinnest areas of joint buttons could start before the crack initiation at the intersections mentioned above. But our study showed that this did not significantly influence the fatigue life of specimens since the bottoms of joint buttons were not load sustaining areas.

For coach-peel tests, stress concentrations on specimens were also at four locations due to deflection of sheet materials: two next to the joint buttons in the bottom sheets and two next to rivet heads in the top sheets, with all at the side close to the bent radius.

Fig. 13 shows the crack initiation and developing locations and possible failure modes. From Fig. 13a, it can be seen that there were three crack initiations and developing routes: (1) cracks initiated at the bottom surface of the top sheet roughly underneath the outer ring of rivet head and developed in a transverse direction and along the sheet thickness direction to the top surface of the top sheet; (2) cracks initiated at the root of joint button and developed in transverse direction and along the sheet thickness direction to the top of the bottom sheet; and (3) cracks initiated at the tip of the pierced hole of the top sheet, developing in a transverse direction and along the sheet thickness direction to the top surface of the top sheet. Based on the applied load and specimen geometry, it can be seen that locations 1 and 3 were subjected to tensile stresses and location 2 was subjected to compression stresses during the fatigue process. The crack initiation and development at location 2 might be caused by local residual tensile stress [11]. The failure of the joints was the result of crack growth competition following the three different routes. For the (2+2) AA5754 stack with the rivet and die combination studied, all joints failed following routes 1 and 3; however, for other stacks and rivet/die combination, failure in the bottom sheet following route 2 did occur. In this study, majority of the joints failed along route 3, as shown in Fig. 13a; however, when there was no crack at location 3 or the crack at location 3 grew very slowly, the joints would fail along route 1, as shown in Fig. 13b.

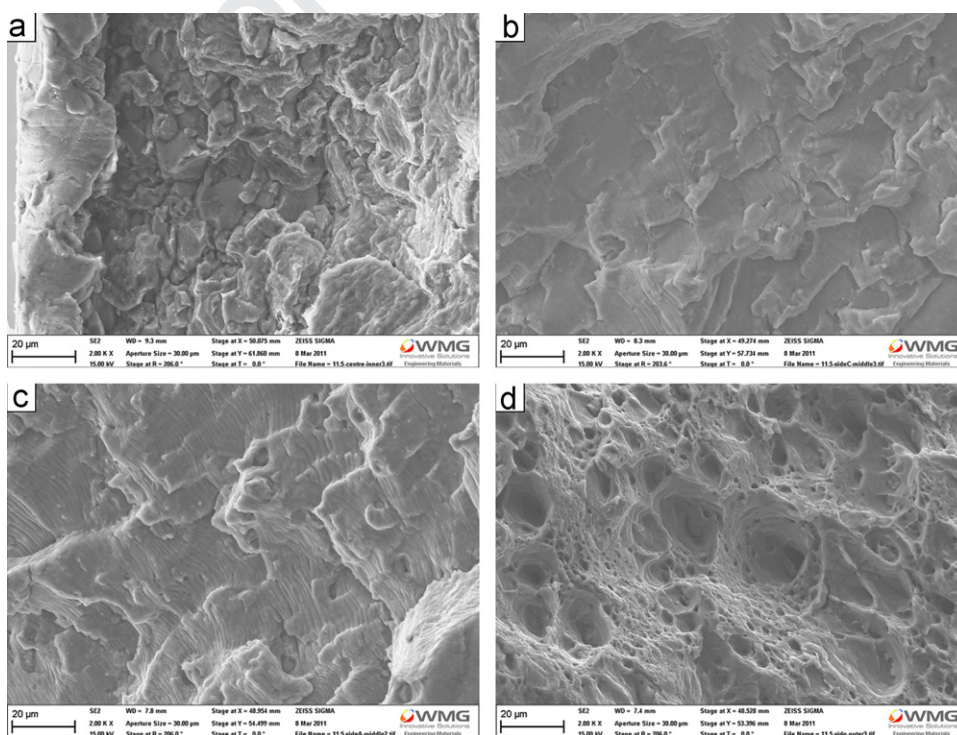
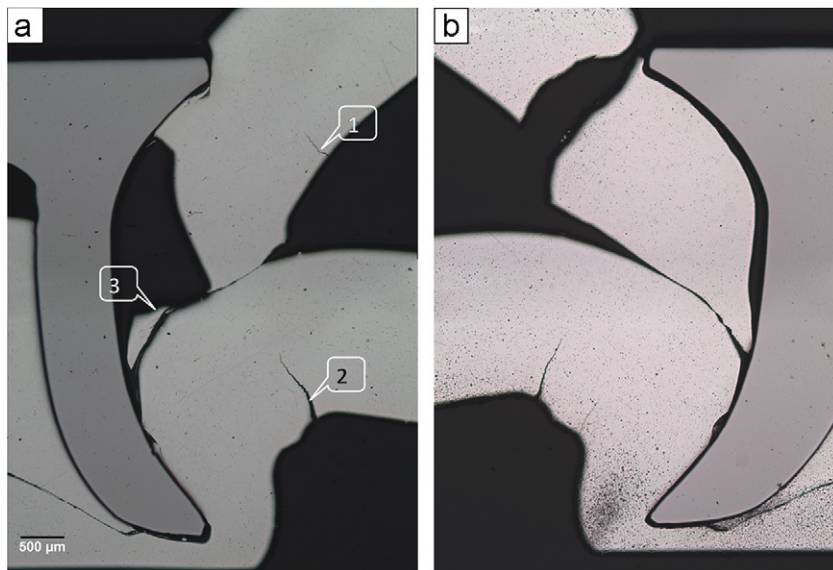


Fig. 12. SEM images of the fracture interface of a lap shear specimen with edge distance as 11.5 mm from areas marked in Fig. 9a: (a) crack initiation, (b, c) crack development and (d) sudden break fracture interface.



**Fig. 13.** Cross-section of failed coach peel specimens with edge distance as 11.5 mm and fatigue tested at load amplitudes of 0.81 kN after 5792 cycles: (a) failure mode 1 with three crack initiation positions (joint 1) and (b) failure mode 2 (joint 2). (Roughly cross-section location indicated by the dash line in Fig. 9a.)

The microstructure of the crack initiation locations can be seen in Fig. 14a. Fig. 14b shows the microstructure of a typical crack growth area, in which two distinct areas from the left side and the right side can be seen. The marked area c and d were enlarged in Fig. 14c and d, respectively. There is a groove with large secondary cracks in areas close to the top surface of the top sheet. This groove started from the hole pierced by the rivet head, and its distance to the top surface of the top sheet increased when it was away from the hole. Force analysis based on specimen geometry shows that the areas on the left side of the groove sustained tensile and shear forces and the areas on the right side (close to top surface) sustained compression and shear forces during fatigue. The **compression-shear** zone crack initiation positions can be seen from Fig. 14b. Basically, it is believed that the crack in the **compression-shear** areas will not significantly influence the fatigue life of specimens. This is because the **compression-shear** area is limited to a very narrow area close to the top surface of top sheet, and this area would have large shear stress for crack initiation only when the primary **tension-shear** cracks had almost fully developed and the sheet lost most of its strength. Fig. 14c shows the typical fracture interface in the **tension-shear** crack development areas. It failed by transgranular fracture and no clear striation marks can be seen. Fig. 14d shows the typical fracture interface in the **compression-shear** crack development areas. It can be seen that this area failed by intergranular fracture. The areas around the groove are transition areas between tension and compression, as shown in Fig. 14d and e. It can be seen that the areas close to the groove on the **tension-shear** side failed by intergranular failure with secondary cracks also developing along grain boundaries. The area close to the groove on the **compression-shear** side was very smooth and striation marks could be seen at higher magnifications. A lot of secondary cracks were found in the **tension-shear** areas, but no secondary crack was seen in the **compression-shear** areas. Fig. 13f shows the final ductile fracture interface when the local stress exceeded the fracture strength of the remaining structure.

#### 4.3. Fatigue life

During a fatigue test of these double riveted specimens, cracks initiated at stress concentration locations (around rivets) and developed along transverse direction and the sheet thickness direction; specimens failed whenever cracks were close to reaching sheet edges or met at the centre of a sheet leaving the joints very weak. Based on

the results from cross-section analysis for crack initiation and growth, it can be seen that for lap shear and coach peel fatigue, cracks initiated at different stages of the fatigue cycles. For lap shear fatigue, cracks initiated at a stage of about 70% of final fatigue life, and for coach peel fatigue, cracks initiated at a stage of about 15–22% of final fatigue life.

Fatigue crack initiation in a ductile metal is a consequence of reversed plasticity within a grain on a scale of  $10^{-3}$  mm. Surface grains are the weakest locations, and they deform plastically at lower stress leading to the production of microcracks within a grain [12]. Such microplasticity, due to slip within grains, can occur at stresses much lower than the tensile yield stress [13]. Since crystal slip is normally caused by shearing, shear stress is very important for crack initiation. Due to the specimen geometry and loading direction during a fatigue test, a coach peel specimen will sustain much more bending and shearing, and as a result, the shear stress along slip planes in a lap shear fatigue specimen is much lower than that in a coach-peel fatigue specimen when a similar load is applied. In this study, it was possible that for coach peel fatigue of specimens with all edge distances, the initial shear stress was much larger than the critical shear stress required for crack initiation for all load amplitudes applied. As a result, when the same load amplitude was applied, specimens with different edge distance tended to initiate cracking very fast after similar cycles and the final fatigue life was mainly influenced by the length of crack development path, although different level of stress concentration for specimens with different edge distances might have some influence. However, for lap shear fatigue, since the shear stress was much lower, the crack initiation period was very long and accounted for 70% of the fatigue life. For specimens with different edge distance, it would take different time for the crack to initiate, since their shear stress was different, and this was the main reason that caused the differences in fatigue life. Although the crack development path length also influenced the fatigue life, in this case this influence was less significant.

For specimens with edge distance of 5–8 mm, because the half distance between the two rivets was not less than the distance between rivets and sheet edges and assuming that cracks grew at the same rate toward sheet edge and sheet centre, the areas between rivets and sheet edges would fail first leaving the central part of the sheet in connection. When edge distance of specimens increased to 11.5 mm, the half distance between two rivets was

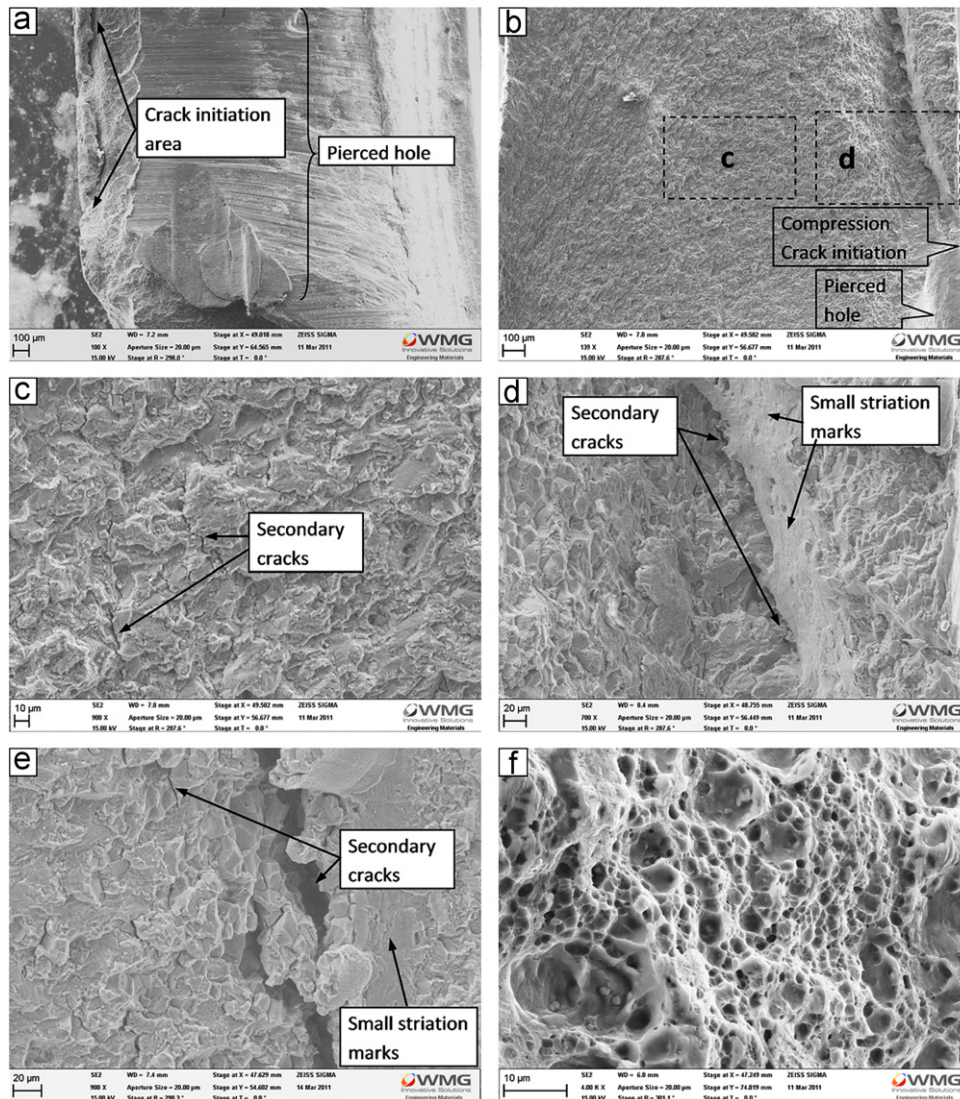


**Fig. 14.** SEM images of the fracture interface of a coach-peel specimen with edge distance as 11.5 mm from areas marked in Fig. 12: (a) crack initiation, (b) a typical fracture interface close to the primary crack initiation location, (c, d) enlarged local areas marked in (b), (e) secondary cracks at the tension/compression interface, and (f) sudden break fracture interface. (The top surface of top sheet is on the right side and bottom surface is on the left side of the images.)

slightly larger than the distance between rivets and sheet edges. In this case, the areas between rivet and sheet edges and the area between two rivets failed almost simultaneously. When the edge distance of specimens increased further to 14.5 mm, all specimens failed at central areas with the areas between rivets and sheet edges still in connection. This was because the cracks developing path length at central areas was shorter than that to sheet edges.

Based on the fatigue lives of specimens with different edge distances and the above analysis, it can be concluded that for coach-peel fatigue, length of crack developing path was the determining factor for fatigue resistance of different specimens. Once cracks grew long enough, the strength of specimens would be lost and the specimen would fail. Specimens with an edge distance of 11.5 mm had the longest crack developing path before they lost their strength, so these specimens had the best fatigue resistance among all specimens studied. For lap shear fatigue, level of stress concentration determined the crack initiation time and eventually determined the fatigue life. For the specimens with edge distance of 11.5 mm, since the two rivets were more evenly located along the width of specimens, stress distribution in specimens was more even. As a result, when same load amplitude

was applied, the maximum shear stress in the specimens with edge distance of 11.5 mm would be smaller than that in the specimens with other edge distances. Consequently, the specimens with edge distance of 11.5 mm would have the longest crack initiation time and fatigue life. Based on lap shear and coach-peel fatigue tests, it can be seen that 11.5 mm is the optimum edge distance for fatigue strength.

## 5. Conclusions

In this paper, the influence of rivet centre to sheet edge distance on the fatigue performance of SPR double joints specimens was studied to optimise structure design for further automotive body weight reduction. The following conclusions can be drawn:

- (1) Edge distance has great influence on lap shear fatigue resistance but it has less significant influence on coach-peel fatigue resistance.
- (2) All specimens failed at sheet material by cyclic bending. For lap shear fatigue tests, specimens failed in the bottom sheet at low load amplitudes and in the top sheet at high load

1 amplitudes except for specimens with very short edge dis-  
2 tance of 5 and 6 mm. For coach-peel fatigue tests, all speci-  
3 mens failed in the top sheet.

- 4 (3) During a fatigue test, cracks initiated at stress concentration  
5 areas around rivet heads or joint buttons.  
6 (4) The failure of coach peel fatigue specimens was the result of  
7 competition between three different crack initiation and  
8 developing routes.  
9 (5) For coach-peel fatigue, length of crack developing path was  
10 the main factor that determined the fatigue life of different  
11 specimens, and for lap shear fatigue, level of stress concen-  
12 tration and subsequent crack initiation time was the main  
13 factor that determined the fatigue life.  
14 (6) An optimum edge distance of 11.5 mm is suggested to achieve  
15 good fatigue performance, and a minimum edge distance of  
16 8 mm is required in order to maintain reasonable fatigue  
17 resistance.

### 19 Acknowledgement

20 The authors would like to thank the European Regional  
21 Development Fund and the Advanced West Midlands Fund, UK,  
22 for the support of this research.  
23  
24  
25

### References

- 27 [1] A.R. Krause, A.R.A. Chernenkoff, SAE World Congress 1995. Paper no. 950710.  
28 [2] G.S. Booth et al., SAE World Congress 2000. Paper no. 2000-01-2681.  
29 [3] M. Zhou, S.J. Hu, H. Zhang, Weld. Res. Suppl. (1999) 305s–313s.  
30 [4] H. Yang, et al., Mater. Design 29 (2008) 1679–1684.  
31 [5] D. Li, et al., Mater. Design 34 (2012) 22–31.  
32 [6] C.P. Fung, J. Smart. Proc. IMech. G 211 (1997) 13–27.  
33 [7] L. Han, A. Chrysanthou, K.W. Young, Mater. Design 28 (2007) 2024–2033.  
34 [8] S. Kalluri, G.R. Halford, M.A. McGaw, Technical Memorandum 106881, 1995,  
35 NASA.  
36 [9] Y.K. Chen, et al., Wear 255 (2003) 1463–1470.  
37 [10] L. Han, A. Chrysanthou, J.M. O'Sullivan, Mater. Design 27 (2006) 200–208.  
38 [11] N.E. Fleck, C.S. Shin, R.A. Smith, Eng. Fract. Mech. 21 (1985) 173–185.  
39 [12] L.P. Pook, Metal Fatigue: What it is, Why it matters?, Springer, Dordrecht,  
40 Netherlands, 2007.  
41 [13] A.H. Cottrell, Theory of Crystal Dislocations, Blackie and Son, London, 1964.